Electro-mediated PhotoRedox Catalysis for Selective C(sp^3)-O Cleavages of Phosphinates to Carbanions

Xianhai Tian,[a] Tobias A. Karl,[a] Sebastian Reiter,[b] Shahboz Yakubov,[a] Regina de Vivie-Riedle,[b] Burkhard König*[a] and Joshua P. Barham*[a]

[a]Universität Regensburg, Fakültat für Chemie und Pharmazie, 93040 Regensburg, Germany

[b]Department of Chemistry, LMU Munich, 81377 Munich, Germany

Abstract We report a novel example of electro-mediated photoredox catalysis (e-PRC) in the reductive cleavage of C(sp^3)-O bonds of phosphinates to alkyl carbanions. As well as deoxygenations, olefinations are reported which are *E*-selective and can be made *Z*-selective in a tandem reduction/photosensitization process where both steps are photoelectrochemically promoted. Spectroscopy, computation and catalyst structural variations reveal that our new naphthalene monoimide-type catalyst allows for a more intimate dispersive precomplexation of its radical anion form with the phosphinate substrate, facilitating a reactivity-determining C(sp^3)-O cleavage. Surprisingly and in contrast to previously reported photoexcited radical anion chemistries, our conditions i) tolerate aryl chlorides/bromides and ii) do not give rise to Birch-type reductions.

Introduction Synthetic methodologies involving single electron transfer (SET) are increasingly popular for the facile synthesis or modifications of important organic compounds. PhotoRedox Catalysis (PRC)[1] and Synthetic Organic Electrochemistry (SOE)[2] lead to easy SET processes, providing notable redox power for various organic transformations under mild conditions. Generally, visible-light PRC generates radical intermediates with good functional group tolerance in a mild manner. However, synthetic applications of PRC in terms of transformations needing highly-oxidizing or reducing potentials are limited by the energetic limitations of visible light photons. One solution is to generate photoexcitable radical ions by multi-photon processes.[3]

Such photoexcited radical ions are highly oxidizing[3a,b] or reducing species,[3c-h] leading to a significantly expanded redox 'window' for activating inert substrates. Sacrificial redox additives (e.g. DIPEA) are employed in stoichiometric excesses in consecutive Photoinduced Electron Transfer (conPET) processes to prime catalysts prior to excitation. Their excesses and organic by-products can plague purification steps. In contrast, SOE allows direct access to high, user-controlled redox energy without involving photocatalysts or sacrificial redox additives, possessing a great advantage for net-oxidative/reductive reactions. However, the applied constant current or voltage can cause uncontrollable over-reductions/oxidations to afford by-products.

To address the aforementioned limitations in PRC and SOE, organic chemists have recently explored their combination.[4] Merging the advantages of these two important techniques has made photoelectrochemistry a tool for greener, more challenging and more selective molecular activations.[5] Pioneering reports by Xu,[5b-c,o] Lambert,[5g,h,i,k] Lin[5h,j] and Wickens[5f] have shown that introducing applied potential in photoredox catalysis is not only beneficial for accessing challenging redox reactions, but is also a green replacement for sacrificial redox additives. Among the various strategies for combining photocatalysis and electrochemistry[4a] the sub-category coined electrochemically-mediated PhotoRedox Catalysis (e-PRC) is highly attractive. In addition to turning over 'spent' closed-shell photocatalysts, e-PRC can also involve electrochemical generation of open-shell (radical ion) photocatalysts, followed by their photoexcitation to species with ultra-high redox potentials.

A seminal report from the Lambert group demonstrated this strategy for super-oxidations of highly electron-poor arenes.[5k] In the reductive direction, photoexcited radical anions of dicyanoanthracene (**DCA**)[5h] and of 2,6-diisopropylphenyl-containing naphthalenemonoimide (**NpMI**)[5f] are highly reducing species (E^{o}_{red} < -3.0 V vs. SCE) that reduce challenging aryl chlorides to their aryl radicals. Even *p*-chloroanisole was reduced, beyond reach of the photon energy limit of monophotonic PRC and where SOE inevitably leads to dehalogenation via subsequent aryl radical reduction (Figure 1A).[6]

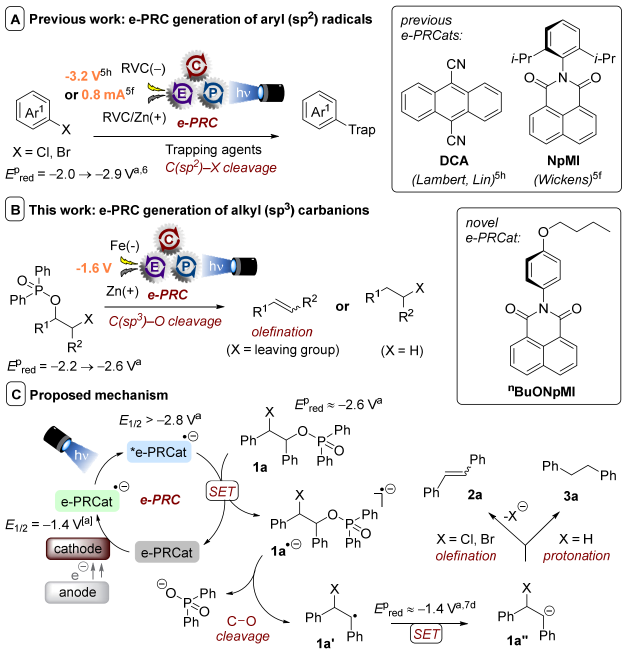

Figure 1. Previous reductive e-PRC reports involving C(sp^2)-X cleavages to afford aryl radicals vs. this work involving C(sp^3)-O cleavages to afford alkyl radicals and carbanions. [a]Redox potentials are vs. SCE.

Despite these elegant advances, reductive e-PRC and biphotonic strategies[3] are still heavily focused on the reductions of aryl halides/pseudohalides through C(sp^2)–X bond cleavages to generate aryl C(sp^2) radicals in an overall dehalogenation or functionalization with excesses of radical trapping agents.[5f,h] Inspired by previous reports,[5] we envisioned that phosphinates of aliphatic alcohols (E^{p}_{red} = -2.2 → -2.6 V vs. SCE) could undergo e-PRC reduction to give carbanions (Figure 1B). Thereby, an electroactivated-PhotoRedox Catalyst (e-PRCat) undergoes cathodic activation and photoexcitation to afford a potent reductant. SET reduction of **1a** to its radical anion followed by C(sp^3)–O bond cleavage delivers benzyl radical **1a'**. Its further reduction[7d] to carbanion intermediate **1a''** would enable either an olefination (X = Cl, Br) or a deoxygenation (X = H) process by a mechanism that depends neither on hydrogen atom transfer agents nor or decarboxylation.[7] Herein, we report the e-PRC reduction of alkyl phosphinates to alkyl(sp^3) carbanions for olefination and deoxygenation reactions that i) proceeds under exceedingly mild conditions, ii) tolerates aryl halides/pseudohalides with similar or more accessible redox potentials than the target alkyl phosphinate moiety.

Synthetic Results To assess the viability of our proposed e-PRC alkyl phosphinate reduction, we employed 2-chloro-1,2-diphenylphosphinate **1a** as a model substrate for the olefination reaction (Table 1). By using **DCA** as an e-PRCat and Zn(+)/RVC(−) as the electrodes in a divided H-cell, we examined the reduction of **1a** under blue light irradiation and with different applied constant potentials. A high constant voltage (U_{cell} = −3.2 V) as used previously[5h] for electron-priming **DCA** to its radical anion for photoexcitation gave notable decomposition, desired product *E*-stilbene (*E*-**2a**) in only 7% yield and a 25% yield of diphenylethane **3a**[8] (Table 1, entry 1). A lower potential (U_{cell}= −1.6 V) led to a remarkable improvement in the reaction profile and yield of *E*-**2a** to 70% (Table 1, entry 2). The optimal yield of *E*-**2a** was obtained at an even lower potential (U_{cell} = −1.0 V). Cyclic phosphate ester **4a** was also a suitable substrate for preparing product *E*-**2a** (entry 4), offering an attractive Corey-Winter-type olefination that avoids explosive/toxic trimethylphosphite, harsh activating reagents or high temperature. Control reactions omitting light, constant potential or e-PRCat confirmed the photoelectrochemical nature of the olefination reaction (entries 5-7). In contrast to **DCA**, **NpMI** as catalyst delivered higher amounts of *Z*-**2a** (entry 8).[9] Allowing the reaction to proceed for 48 h (entry 9) increased the *E*-/*Z*- ratio to 1/10 (71% of *Z*-**2a**). Detailed investigations (see Supporting Information (SI)) revealed that light, constant potential and **NpMI** are all advantageous to the isomerization process, representing a novel photoelectroisomerism of alkenes.

Reaction scope was expanded to other substrates including precursors to unsymmetrical stilbenes as well as cyclic, hindered and terminal olefins. Phosphinate precursors are readily synthesized from their ketones via α-chlorination and one-pot $NaBH_4$ reduction/Cl-P(O)Ph_2 protection (see SI). Here we opted for Fe instead of RVC as a cheaper, robust cathode material.[10] However, it was quickly identified that **DCA** and **NpMI** were ineffective e-PRCats for the majority of phosphinates. For example, cyclic substrate **1d** underwent no reaction with these catalysts (entries 10-11).

Table 1. Optimization of the reaction conditions[a]

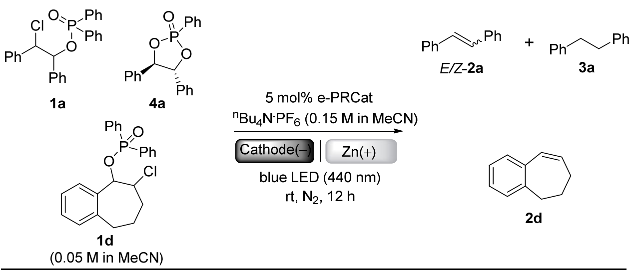

entry	substrate	e-PRCat	U_{cell} /V	t /h	product: yield[a]
1	1a	**DCA**	−3.2	12	**2a**: 7% *E*-/*Z*- > 20:1[b] **3a**: 25%
2	1a	**DCA**	−1.6	12	**2a**: 70% *E*-/*Z*- > 20:1[b] **3a**: trace
3	1a	**DCA**	−1.0	12	**2a**: 79% *E*-/*Z*- > 20:1[b] **3a**: n.d.
4	4a	**DCA**	−1.	24	**2a**: 79% *E*-/*Z*- > 20:1[b] **3a**: n.d.
5[c]	1a	**DCA**	−1.0	12	**2a**: n.d. **3a**: n.d.
6	1a	**DCA**	-	12	**2a**: n.d. **3a**: n.d.
7	1a	**-**	−1.0	12	**2a**: trace **3a**: n.d.
8	1a	**NpMI**	−1.6	12	**2a**: 80% *E*-/*Z*- = 1:1.3[b] **3a**: n.d.
9	1a	**NpMI**	−1.6	48	**2a**: 78% *E*-/*Z*- = 1:10[b] **3a**: n.d.
10[d]	1d	**DCA**	−1.0	12	**2d**: n.d.
11[d]	1d	**NpMI**	−1.6	12	**2d**: trace
12[d]	1d	**^{n}BuO-NpMI**	−1.6	12	**2d**: 75%
13[d]	1d	**^{n}BuO-NpMI**	-	12	**2d**: n.d.
14[c,d]	1d	**^{n}BuO-NpMI**	−1.6	12	**2d**: n.d.
15[d]	1d	**^{n}BuO-NpMI**	−1.6	12	**2d**: < 5%

n.d., not detected; [a]Yields determined by ^{1}H NMR spectroscopy with 1,3,5-trimethoxybenzene as an internal standard; [b]*E*-/*Z*- ratios determined by ^{1}H NMR; [c]in the dark; [d]Fe cathode.

We synthesized **ⁿBuO-NpMI** as a novel e-PRCat which afforded the desired product **2d** in very good yield (entry 12). Control reactions confirmed operation of e-PRC (entries 13-15), while cathode materials greatly impacted the reaction (for detailed optimizations, see SI).[11] Optimal conditions were examined for a range of olefination reactions (Figure 2). Unsymmetrical *Z*-stilbenes **2b**-**2c** were prepared in high yields from the tandem e-PRC reduction/photoelectroisomerism process. Cyclic olefins **2d**-**2h**, rarely synthesized by the Wittig reaction due to the inconvenience of substrate preparations, were prepared in good to excellent (69-83%) yields. Terminal olefin **2i** could not be prepared in high selectivity by dehydration of its corresponding tertiary alcohol as such a method inevitably leads to the most substituted olefin,[12] in this case, a tetrasubstituted instead of a terminal olefin. After the successful preparations of a series of *E*-styrene derivatives (exclusive isomers) bearing divergent substituents including -Ph (**2j**), -OBz(**2k**), -OMe(**2l**) and -CF_3(**2n**) at their arene rings, we questioned whether halogen substituents could be tolerated by our reaction. This is a highly challenging issue, since the reductions of aryl chlorides and bromides by photoexcited radical anions (either e-PRC or conPET-type) are highly efficient and heavily reported as discussed earlier (Figure 1A).[3c-g,5f,5h] With this aim, we tested phosphinates bearing either a chloro- or bromo- substituent on their arene. To our delight, aryl chlorides **1o**-**1q** and aryl bromide **1r** underwent olefination in moderate to good (39-69%) yields with high or exclusive selectivities for their *E*- or *Z*- isomers; only traces of dehalogenated styrenes were observed (>10:1 in favor of olefination for **2p**). Compared with products **2o**-**2p**, *p*-chlorostilbene **2q** has a more conjugated π-system and is easier to reduce, yet still gave only traces of dechlorinated product **2a**. Substrate **1s**, bearing both an alkyl and aryl phosphinate,[13] selectively underwent e-PRC reduction of the alkyl phosphinate leading only to C(sp^3)-O cleavage to afford **2s** in good yield. Our method provides complementary selectivity to a recent report involving a phenothiazine photocatalyst.

Styrene-forming substrates containing longer-chain aliphatic groups or a benzyl group retained high *E*-isomer selectivity, affording **2t**-**2v** in good to high (62-79%) yields and high selectivities (>10:1 in favor of their *E*-isomers). Hindered olefins derived from carbocycles **1w**-**1x** were formed in high (83-87%) yields. In the synthesis of **2x**, our conditions offer an alternative to i) ⁿBuLi or Grignard chemistry with expensive bromocyclobutane and ii) expensive Wittig reagents/cyclobutanone, instead starting from commercial, inexpensive cyclobutyl phenyl ketone. Our e-PRC phosphinate reduction offers complementary selectivity to Birch-type photochemical reports involving SET,[14] or E_nT.[15] Naphthalene-based substrate **1y** was well-tolerated, affording **2y** in good (62%) yield without Birch-type reduction products. Amide **1z** was also well-tolerated, in spite of its free proton and labile heterocycle that would react with strong bases. Although an alkyl phosphinate derived from a non-benzylic alcohol **1aa** did not react, alkyl phosphinates derived from allylic alcohols were feasible. Allylic substrates **1ab**-**1ac** derived from naturally-occurring terpenes were found to be sluggish, but afforded dienes **2ab**-

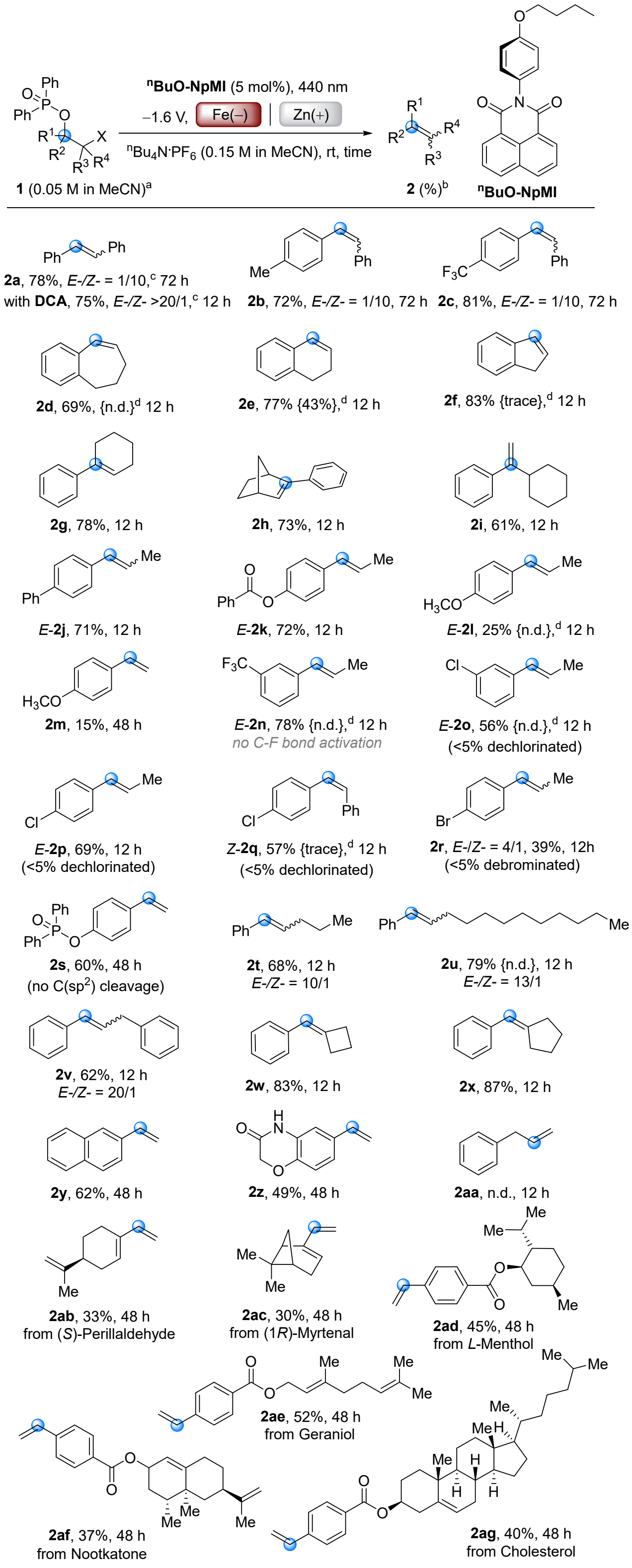

Figure 2. e-PRC reductive olefination scope. [a]for compounds **2a-2q**, **2t-2x**, **2aa-2ad**, X = Cl; for compounds **2r-2s**, **2y-2z**, **2ae-2ag**, X = Br; [b]Isolated yields; [c]*E*-/*Z*- ratios determined by ^{1}H NMR; [d]Yields in parenthesis {} are ^{1}H NMR yields from **NpMI** as an e-PRCat.

2ac in satisfactory (30-33%) yields in a complementary fashion to previous reports that require strong bases[16] or transition metal catalysis.[17] Demonstrating the utility of our base-free approach, products **2ad**-**2ag** were synthesized from their alkyl *p*-acetylbenzoate precursors. Given the properties of Geraniol and Nootkatone as fragrance oils and cholesteryl benzoate as a liquid crystal, our reaction is a useful entry to terpene-loaded monomers for the synthesis of functional polymers.[18] Strategies involving strong base - for example i) Wittig reaction of an aldehyde or ii) ketone reduction, mesylation and E_2-elimination - lead to hydrolysis or E_2 elimination of the benzoate,[19] while direct esterification suffers from the caveats that 4-vinylbenzoic is thermally sensitive and formulated with BHT stabilizer. Further exemplifying utility, substrate **1ah**, readily prepared from its α-dichloroketone, underwent selective reduction to its unsymmetrical stilbene **2ah** in good yield while leaving the olefinic Cl atom untouched (Figure 3). This demonstrates the value of our method which retains reductively-labile halides for further functionalizations. The method provides alternative access to unsymmetrical halogenated stilbenes that does not rely on transition metal catalysis.[20] While conPET photocatalysis and e-PRC are complementary approaches in the reductions of aryl halides/pseudohalides,[3f,g] conPET conditions did not effect the net-reductive transformation herein (Figure 4).

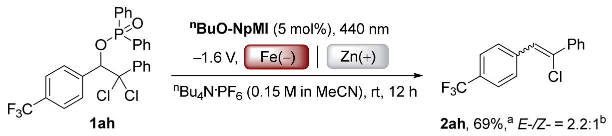

aYield of isolated product, bE-/Z- ratio determined by ^{1}H NMR.

Figure 3. e-PRC reduction of dechlorinated substrate.

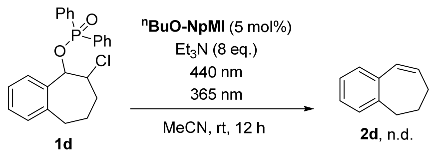

Figure 4. Reduction attempt using conPET conditions.

At this juncture, we wondered if overall deoxygenation would be possible by removing the α-Cl atom from **1a** (**1ai**) as the generated carbanion would be protonated. Direct electrolytic reduction of alkyl phosphinates is known, and required a constant current of 600 mA at 60-110 °C where a constant potential (U_{cell} = −2.4 V vs. Ag/AgCl) was ineffective.[21] Reductive functionality (styrenes, aryl halides, dienes, benzoates) would not tolerate these conditions. e-PRC deoxygenation afforded desired product **1ai** in good yield under standard conditions (U_{cell} = −1.6 V) with extended time (Figure 5). Allylic substrate **1aj** smoothly deoxygenated to **2aj** (Limonene). When a Cl atom was present β- to the phosphinate (**1ak**), deoxygenation afforded **2ak** and cyclopropane **2ak'**, confirming the intermediacy of a benzylic carbanion (see **1a''**, Figure 1C). An alkyl phosphinate derived from a non-benzylic/allylic alcohol (**1al**) did not react.

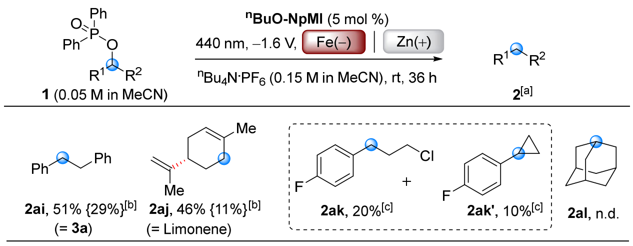

Figure 5. e-PRC reductive deoxygenation. Isolated yields of products **2ai** and **2aj**; bYields in parenthesis {} are ^{1}H NMR yields from using NpMI as an e-PRCat; cYields of **2ak** and **2ak'** are by ^{1}H NMR with 1,3,5-trimethoxybenzene as an internal standard, identified by literature comparisons and GC-MS traces.

Mechanistic Studies We sought explanations as to two questions: 1) why e-PRC conditions herein could not engage non-benzylic substrates (**1aa** and **1al**, respectively) and 2) why **ⁿBuO-NpMI** was a superior e-PRCat to **NpMI**; since **NpMI** as an e-PRCat gave no conversion of various substrates (**1f**, **1n**, **1o**, **1q**, **1u**) in olefinations (Figure 2), and poor conversion of **1ai** and **1aj** in deoxygenations (Figure 5).

Table 2. Calculated properties of phoshinate radical anions vs reactivity.

entry	radical anion	e-PRCat	yield (%)a	BDFE (kcal/mol)b	E^{p}_{red} (V) calc.c,exp.d
1	1g	**NpMI**	78 (**2g**)	−39.8 (C-O)	−2.55,−2.47
2	1a	**NpMI**	78 (**2a**)e	−39.2 (C-O)	−2.60,−2.23 /−2.34
3	1ai	**ⁿBuO-NpMI**	51 (**2ai**)	−38.7 (C-O)	−2.55, -
4	1o	**ⁿBuO-NpMI**	56 (**29o**)	−38.1 (C-O)	−2.45,−2.60
5	1o	**ⁿBuO-NpMI**	5 (de-Cl)	−26.9 (C-Cl)	- ,−2.78f
6	1r	**ⁿBuO-NpMI**	39 (**2r**)	−38.2 (C-O)	−2.44,−2.33 /−2.46
7	1r	**ⁿBuO-NpMI**	trace (de-Br)	−30.6 (C-Br)	- ,−2.44f
8	1d	**ⁿBuO-NpMI**	39 (**2r**)	−34.5 (C-O)	−2.44,−2.41
9	1aa	**ⁿBuO-NpMI**	39 (**2r**)	−27.5 (C-O)	−2.40,−2.42
10	1al	**ⁿBuO-NpMI**	39 (**2r**)	−22.1 (C-O)	−2.56,−2.68

aProduct yields as defined in Figures 2 and 5; bbond dissociation free energies (ΔG) calculated at the ωB97X-D/6-311+G*, IEFPCM(MeCN) theory level; ccalculated at the ωB97X-D/6-311+G*, IEFPCM(MeCN) theory level and calibrated to an experimental set, see SI; dmeasured at 10 mM [phosphinate] in 0.1 M ^{n}Bu$_4$N·PF$_6$ in MeCN using Fc as an internal standard and calibrated vs. SCE, see SI; fLiterature redox potentials of PhCl and PhBr are taken as surrogates.[6]

Concerning the first question, measured reduction potentials (E^{p}_{red}) of the alkyl phosphinates - in good agreement with those calculated by DFT - did not correlate with reactivity (Table 2). Instead, comparison of the C(sp^3)-O bond-dissociation free energies (BDFEs) of phosphinate radical anions correlated well with reactivity. This corroborated C(sp^3)-O cleavage as the rate-limiting step and rationalized i) the unique tolerance of our conditions to aryl halides due to their less exergonic C-X BDFEs (entries 4,5; 6,7) and ii) the lack of reactivity of phosphinates derived from non-benzylic/allylic alcohols that require higher temperatures[21] to assist C(sp^3)-O cleavage (entries 9,10). As to the second question, **NpMI** and **ⁿBuO-NpMI** had identical redox potentials ($E_{1/2}$ = −1.3 V vs. SCE, Figure 6, left) by cyclic voltammetry. Their radical anions are electrogenerated with equal efficiency, which is entirely consistent with the spin densities of their radical anions (Figure 6, right) being localized on the naphthalene and being unaffected by substitution on the *N*-aniline. Spectroelectrochemistry of both e-PRCats gave identical UV-vis bands for their radical anions (Figure 7, left and see SI). Taken together, these results indicate that their excited radical anions are equally potent reductants. To probe further, we electrochemically generated **NpMI•⁻** and **ⁿBuO-NpMI•⁻** under inert conditions for analysis by EPR (Figure 7, right).[22]

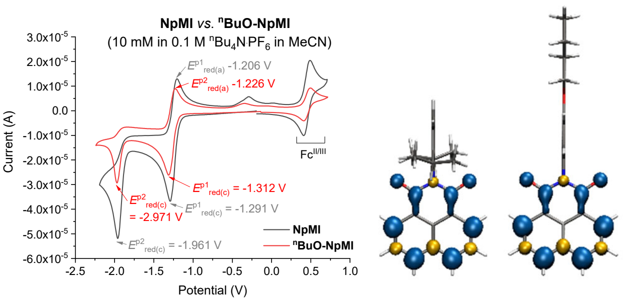

Figure 6. Cyclic voltammetry of e-PRCats (10 mM [e-PRCat] in 0.1 M $^nBu_4N{\cdot}PF_6$ in MeCN) vs. Ag/AgCl (left). DFT calculated spin densities of **NpMI•⁻** and **ⁿBuO-NpMI•⁻** (right), see SI for details.

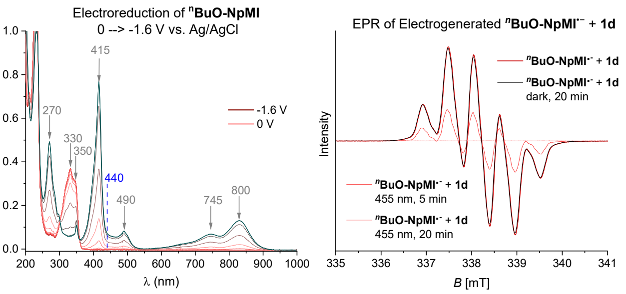

Figure 7. Spectroelectrochemistry of **ⁿBuO-NpMI** (2.5 mM in 0.1 M $^nBu_4N{\cdot}PF_6$ in MeCN) from 0 to −1.6 V vs. Ag/AgCl (left). EPR spectrum of electroreduced **ⁿBuO-NpMI** (2.5 mM in 0.1 M $^nBu_4N{\cdot}PF_6$ in MeCN at U_{cell} = −1.6 V for 1 h) in the presence of **1d** (10 eq.) and signal quenching upon light irradiation (right).

In both cases, a pentet was observed whose intensity was unchanged upon irradiation with blue LEDs. In both cases, in the presence of **1d** (10 eq.), the EPR signal was identical in the dark (see SI), but upon irradiation by blue LEDs the EPR signal quenched, corroborating successful SET from the doublet states (D_n) of both catalysts ^{2}[**NpMI•⁻***] and ^{2}[**ⁿBuO-NpMI•⁻***] to **1d**. Given that the reaction of **1d** is only successful with **ⁿBuO-NpMI•⁻** and taken together with the discussion of E^p_{red}s and BDFEs in Table 2, this confirms SET is not the determining factor for the success of **ⁿBuO-NpMI•⁻**. Neutral and electroreduced forms of **NpMI** and **ⁿBuO-NpMI** were probed by luminescence spectroscopy (Table 3). For neutral e-PRCats, measured lifetimes (τ = 3.0 ns) aligned with the literature.[23] Since singlet (S_1) states of *N*-arylnaphthalimides are ultrashort lived, intersystem crossing is known to occur[23] and recorded lifetimes are assigned to triplet states of similar analogs (T_1).[23] Electroreduction for 1 h and selective excitation of the radical anions at 452 nm led to a new emission band (λ_{max} ca. 540 nm) and a longer-lived species for both **NpMI•⁻** and **ⁿBuO-NpMI•⁻** that displayed biexponential luminescence decay (τ_1 = ~7; τ_2 = ~20 ns in both cases). Intersection of the longest wavelength absorption and shortest wavelength emission bands allows an estimation of $E^{0\text{-}0}$ for photoexcited states.[24] For these emitting excited states, $E^{0\text{-}0}$ values (E^{ES}) for both [**NpMI•⁻***] and [**ⁿBuO-NpMI•⁻***] were (E^{ES} = 56.6 kcal/mol) almost identical to the triplet energies (E^T) of *Ir^{III} photosensitizers used in olefin photoisomerisms.[9b-c] It is therefore reasonable to propose *E*-/*Z*- photoisomerism occurs via energy transfer (E_nT) from this longer-lived excited state of [**ⁿBuO-NpMI•⁻***]. E_nT is exergonic to *E*-stilbene and less so to *Z*-stilbene (E_T = 51.0 vs. E_T = 55.5 kcal/mol, respectively), rationalizing high *Z*-stilbene selectivity.[9b,c,25] However, the lifetime of this state was unchanged in the presence of **1d** (10 eq.), confirming its catalytic inactivity in the initial SET step.

Table 3. Lifetimes of neutral vs. electroreduced[a] e-PRCats

entry	e-PRCat	conditions	λ_{max} (ex)	λ_{max} (em)	$E^{T/ES}$ (kcal /mol)
1	**NpMI**	-	375	412	(T_1) 74.5
2	**NpMI**	−1.6 V, 1 h[a]	452	535	(ES_1) 56.6
3	**ⁿBuO-NpMI**	-	375	412	(T_1) 75.6
4	**ⁿBuO-NpMI**	−1.6 V, 1 h[a]	452	548	(T_1) 56.6
5	**ⁿBuO-NpMI**	−1.6 V, 1 h[a] +10 eq. **1d**	452	548	-

[a]Electroreduced e-PRCat (2.5 mM in MeCN (0.1 M $^nBu_4N{\cdot}PF_6$), diluted 8x.

In their study of photoexcited benzo[*ghi*]perylenemonoamide (BPI) radical anions for Birch reductions, Miyake and co-workers made similar observations.[14] They assigned the long-lived excited state as the lowest-lying quartet excited state (^{4}**BPI•⁻***) arising from intersystem crossing (ISC) from the doublet state (^{2}BPI•⁻*). The lowest-lying quartet state ^{4}[**ⁿBuO-NpMI•⁻***] could be a candidate for the luminescent excited state that effects photoisomerism herein. However, Miyake found that the long-lived excited state was not catalytically active in the Birch SET step. They hypothesized SET from a higher lying excited doublet state ^{2}**BPI**$^{\bullet-*}$ (D_n) in an anti-Kasha fashion. Consistent with previously reported anti-Kasha photochemistry of doublet excited state photocatalysts,[5a,14] excitation of the broad absorption of **^{n}BuO-NpMI$^{\bullet-}$** between 650-900 nm ($D_0 \rightarrow D_1$) with 740 nm or 850 nm LEDs gave only traces of **2d**.[26] Ruling out participation of the first excited state (D_1), we predict 'effective minimum' potentials of **NpMI**$^{\bullet-*}$ (D_n) at −3.7 V vs. SCE and **^{n}BuO-NpMI**$^{\bullet-*}$(D_n) at −3.8 V vs. SCE from the Rehm-Weller equation,[27] easily reaching E^p_{red} of all phosphinates herein as well as aryl halides.[28,29] Participation of a doublet excited state in SET is consistent with aforementioned quenching of the EPR signal (Figure 7, right). High-level DFT/MRCI calculations were carried out for **^{n}BuO-NpMI$^{\bullet-}$** to characterize this D_n state. The computed spectrum (Figure 8, top) is in excellent agreement with the experimental absorption spectrum, especially at the band with λ_{max} = 415 nm comprising two bright π-π* states ($D_0 \rightarrow D_n$ and $D_0 \rightarrow D_{n+1}$). Contrary to the $D_0 \rightarrow D_1$ transition around 870 nm, both these excitations transfer electron density from the naphthalene to the *N*-aniline unit of **^{n}BuO-NpMI$^{\bullet-}$** (Figure 8, bottom). Since the doublet (D_1) states of similar radical anions (naphthalene diimide radical anions, perylene diimide radical anions) are picosecond-lived and do

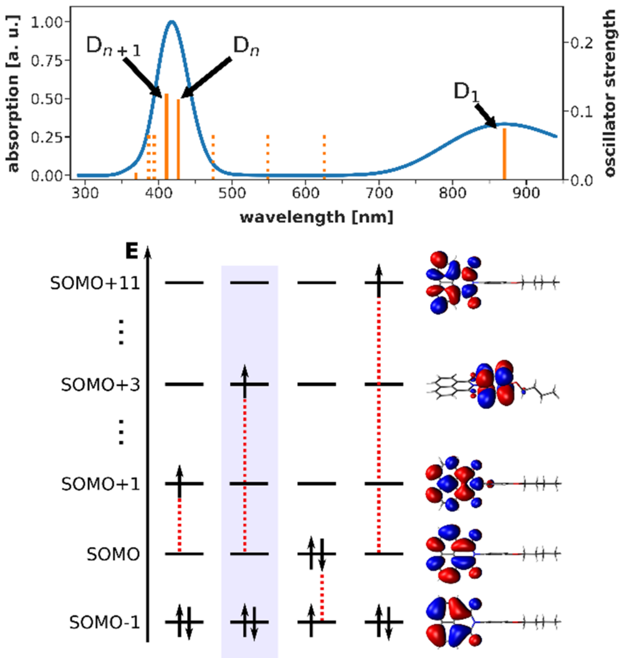

	MRCI weights				λ [nm]	f
D_1	0.86	0.00	0.00	0.00	870	0.0756
D_n	0.00	0.47	0.22	0.15	426	0.1179
D_{n+1}	0.00	0.39	0.13	0.31	410	0.1263

Figure 8. Calculated DFT/MRCI absorption spectrum for **^{n}BuO-NpMI$^{\bullet-}$** (top). Dark states with oscillator strengths f < 0.01 are indicated by dotted orange lines. Leading electronic configurations for the bright excited states D_1, D_n and D_{n+1} (bottom). Dotted red lines indicate single electron excitations from the ground state configuration.

not luminesce,[30] preassembly of ground state radical anion and substrate could explain photochemistry faster than rates of diffusion. Preassembly of **^{n}BuO-NpMI$^{\bullet-}$** with **1d** being more favorable than that of **NpMI$^{\bullet-}$** may explain the reactivity differences of the e-PRCats in effecting C(sp^3)-O cleavage following SET, and may rationalize profound shift in the molecular site of reduction compared to previous reports.[31] However, like Miyake and co-workers, we were unable to find spectroscopic evidence of preassembly by UV-vis or EPR (see SI). While the absence of spectroscopic perturbations does not rule out a preassociation,[32] preassembly could occur at the *N*-aniline that is spin-disconnected from the naphthalene where the radical anion spin density is localized (Figure 6, right). Spin densities of favorable candidate preassemblies at the *N*-aniline unit of **^{n}BuO-NpMI$^{\bullet-}$** found by computational geometry optimizations do not differ from that of **^{n}BuO-NpMI$^{\bullet-}$** alone, while a favorable candidate preassembly at the naphthalene unit of **^{n}BuO-NpMI$^{\bullet-}$** does differ (see SI). A preassembly at the *N*-aniline could also rationalize anti-Kasha photochemistry, since charge transfer to the *N*-aniline in the $D_n/_{n+1}$ states is proximal to the bound substrate and promotes intermolecular SET upon photoexcitation (Figure 8, bottom). In contrast, the charge density of the lowest excited doublet state D_1 remains localized on the naphthalene and is not close to the substrate.

Where spectroscopy offers little insight, a top-down approach varying catalyst structure and examining product yields has proven useful in investigating the mechanisms of reactions involving in situ formed organic electron donors.[33] To probe the importance of a preassembly of **1d** at the *N*-aniline of the e-PRCat, we explored the influence of a series of e-PRCats with varying electronics and steric bulk (**5a-f**, Figure 9). Compared to **NpMI**, catalysts with electron donating alkoxy or *p*-anisole substituents on the naphthalene unit (**5a**,**5b**) gave no reaction. Compared to **^{n}BuO-NpMI**, a catalyst with additional alkoxy substituents on the *N*-aniline (**5c**) gave a lower (41%) yield of **2d**. The yield of **2d** increased with decreasing steric hindrance at the *ortho*-positions of the *N*-aniline (**NpMI**<<**5d**<**5e**). A decrease in 'steric bulk' likely promotes preassociation of radical anion e-PRCat and **1d**.

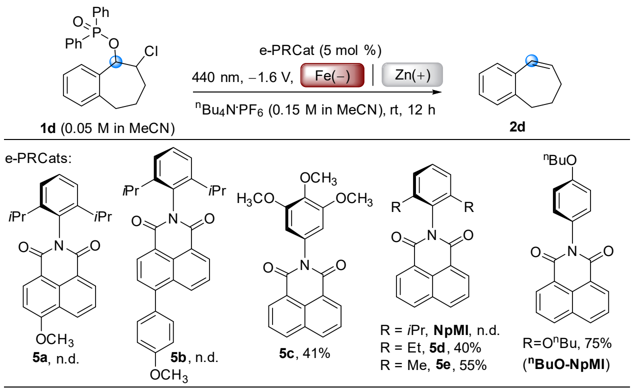

Figure 9. e-PRC deoxygenation of **1d** with various e-PRCats. Yields of **2d** determined by ^{1}H NMR with 1,3,5-trimethoxybenzene as an internal standard.

In our computational investigations we found multiple stable ground state preassemblies. Geometry optimizations (see SI) converged to pincer-like conformations for all candidates, where two of the substrate's aryl groups coordinate to the *N*-

aniline of the e-PRCat in a T-π and π-π orientation, respectively. The thermodynamics and kinetics of their formations (see SI) mirror reactivity trends in Figure 9, corroborating a preassembly between e-PRCat and substrate before photoexcitation.

Conclusion We report an electro-mediated photoredox catalytic reductions of phosphinates derived from α-chloroketones toward selective olefinations and deoxygenations. This study reports reductive formation of alkyl carbanions via photoexcited radical anions as super-reductants. The selective reduction of C(sp^3)-O bonds in the presence of C(sp^2)-X bonds was achieved. Reactivity differences of various radical anion photocatalysts and anti-Kasha photochemistry, backed by computational insights, suggest the importance of a close catalyst-substrate interaction for an effective, selective reaction. In this context, our calculations indicate that intramolecular charge transfer in the catalyst radical anion upon photoexcitation promotes SET to the substrate. Photocatalyst-substrate preassemblies such as EDA complexes,[34] non-covalent interactions,[5a,35] hydrogen bonding[36] and ordering of solvent[37] are receiving increasing attention to unveil the next generation of photocatalytic transformations and offer new frontiers in selectivity and efficiency. Further studies into the nature of interactions and structure of preassemblies are ongoing.

Acknowledgements We thank the Alexander von Humboldt Foundation for funding, provided within the framework of the Sofja Kovalevskaja Award endowed by the German Federal Ministry of Education and Research. We thank Regina Hoheisel for measuring spectroelectrochemistry and cyclic voltammetry. We thank Prof. Patrick Nuernberger, Sebastian Bergwinkl, Stephan Muth, Prof. Robert Wolf and Julia Märsch for assistance and training on glovebox preparations and FT-IR measurements. We thank Prof. John C. Walton for discussions on EPR spectroscopy. T.K. thanks the Deutsche Bundestuftung Umwelt (DBU) for a graduate scholarship. S. Y. is grateful for funding provided by a DAAD scholarship and thanks the SynCat programme of the Elite Network of Bavaria. R.dV-R. and S.R. acknowledge funding by the German Research Foundation (DFG) under Germany's excellence strategy EXC 2089/1 – 390776260. S.R. thanks the International Max Planck Research School on Advanced Photon Science (IMPRS-APS).

References

(1) Selected reviews on photochemistry: (a) Marzo, L.; Pagire, S. K.; Reiser, O.; König, B. Visible-Light Photocatalysis: Does It Make a Difference in Organic Synthesis? *Angew. Chem. Int. Ed.* **2018**, *57*, 10034-10072; (b) Xie, J.; Jin, H.; Hashmi, A. S. K. The recent achievements of redox-neutral radical C-C cross-coupling enabled by visible-light. *Chem. Soc. Rev.* **2017**, *46*, 5193-5203; (c) Romero, N. A.; Nicewicz, D. A. Organic Photoredox Catalysis. *Chem. Rev.* **2016**, *116*, 10075-10166; (d) C. K. Prier, D. A. Rankic, D. W. C. MacMillan, Visible Light Photoredox Catalysis with Transition Metal Complexes: Applications in Organic Synthesis. *Chem. Rev.* **2013**, *113*, 5322-5363.

(2) Selected general reviews on electrochemistry: (a) Meyer, T. H.; Choi, I.; Tian, C.; Ackermann, L. Powering the Future: How Can Electrochemistry Make a Difference in Organic Synthesis? *Chem*, **2020**, *6*, 2484-2496; (b) Xiong, P.; Xu, H.-C. Chemistry with Electrochemically Generated N-Centered Radicals. *Acc. Chem. Res.* **2019**, *52*, 3339-3350; (c) Tang, S.; Liu, Y.; Lei, A. Electrochemical Oxidative Cross-coupling with Hydrogen Evolution: A Green and Sustainable Way for Bond Formation. *Chem.* **2018**, *4*, 27-45; (d) Wiebe, A.; Gieshoff, T.; Möhle, S.; Rodrigo, E.; Zirbes, M.; Waldvogel, S. R. Electrifying Organic Synthesis. *Angew. Chem. Int. Ed.* **2018**, *57*, 5594-5619; (e) Yan, M.; Kawamata, Y.; Baran, P. S. Synthetic Organic Electrochemical Methods Since 2000: On the Verge of a Renaissance. *Chem. Rev.* **2017**, *117*, 13230-13319.

(3) For selected representative examples, see: (a) Tagros, K.; Williams, O. P.; Wickens, Z. Unveiling Potent Photooxidation Behavior of Catalytic Photoreductants. *J. Am. Chem. Soc.* **2021**, *143*, 4125-4132; (b) Rombach, D.; Wagenknecht, H.-A. Photoredox Catalytic a-Alkoxypentafluorosulfanylation of a-Methyl- and a-Phenylstyrene using SF_6. *Angew. Chem. Int. Ed.* **2019**, *59*, 300-303; (c) Neumeier, M.; Sampedro, D.; Májek, M.; de la Peña O'Shea, V. A.; Jacobi von Wangelin, A.; Pérez-Ruiz, R. Dichromatic Photocatalytic Substitutions of Aryl Halides with a Small Organic Dye. *Chem. Eur. J.* **2018**, *24*, 105-108; (d) Ghosh, I.; König, B. Chromoselective Photocatalysis: Controlled Bond Activation through Light-Color Regulation of Redox Potentials. *Angew. Chem. Int. Ed.* **2016**, *55*, 7676-7679; (e) Ghosh, I.; Ghosh, T.; Bardagi, J. I.; König, B. Reduction of aryl halides by consecutive visible light induced electron transfer processes. *Science* **2014**, *346*, 725-728; (f) Li, H.; Tang, X.; Pang, J. H.; Wu, X.; Yeow, E. K. L.; Wu, J.; Chiba, S. Polysulfide Anions as Visible Light Photoredox Catalysts for Aryl Cross-Couplings. *J. Am. Chem. Soc.* **2021**, 143, 481-487. For full reviews, see: (g) Glaser, F.; Kerzig, C.; Wenger, O. S. Multi-Photon Excitation in Photoredox Catalysis: Concepts, Applications, Methods. *Angew. Chem. Int. Ed.* **2020**, *59*, 10266-10284. (h) Castellanos-Soriano, J.; Herrera-Luna, J. C.; Díaz, D. D.; Jiménez, M. C., Pérez-Ruiz, R. Recent applications of biphotonic processes in organic synthesis. *Org. Chem. Front.* **2020**, 7, 1709-1716.

(4) For a full review on the combination of photoredox catalysis and organic electrochemistry: (a) Barham, J. P.; König, B. Synthetic Photoelectrochemistry. *Angew. Chem. Int. Ed.* **2020**, *59*, 11732-11747. For highlights and reviews including this topic: (b) Liu, J.; Lu, L.; Wood, D.; Lin, S. New Redox Strategies in Organic Synthesis by Means of Electrochemistry and Photochemistry. *ACS Cent. Sci.* **2020**, *6*, 1317-1340; (c) Capaldo, L. Quadri, L. L., Ravelli, D. Merging Photocatalysis with Electrochemistry: The Dawn of a new Alliance in Organic Synthesis. *Angew. Chem. Int. Ed.* **2019**, *58*, 17508-17510; (d) Y. Yu, P. Guo, J.-S. Zhong, Y. Yuan, K.-Y. Ye, Merging photochemistry with electrochemistry in organic synthesis. *Org. Chem. Front.* **2020**, *7*, 131-135.

(5) For recent examples on homogeneous photoelectrochemistry, see: (a) Wu, S.; Žurauskas, J.; Domański, M.; Hitzfeld, P. S.; Butera, V.; Scott, D. J.; Rehbein, J.; Kumar, A.; Thyrhaug, E.; Hauer, J.; Barham, J. P. Hole-mediated photoredox catalysis: tris(*p*-substituted)biarylaminium radical cations as tunable, precomplexing and potent photooxicants. *Org. Chem. Front.* **2021**, *8*, 1132-1142; (b) Xu, P.; Chen, P.-Y.; Xu, H.-C. Scalable Photoelectrochemical Dehydrogenative Cross-Coupling of Heteroarenes with Aliphatic C−H Bonds. *Angew. Chem. Int. Ed.* **2020**, *59*, 14275-14280; (c) Lai, X.-L.; Shu, X.-M.; Song, J.; Xu, H.-C. *Angew. Chem. Int. Ed.* Electrophotocatalytic Decarboxylative C−H Functionalization of Hetereoarenes. **2020**, *59*, 10626-10632; (d) Niu, L.; Jiang, C.; Liang, Y.; Liu, D.; Bu, F.; Shi, R.; Chen, H.; Chowdhury, A. D.; Lei, A. Manganese-Catalyzed Oxidative Azidation of C(sp^3)−H Bonds under Electrophotocatalytic Conditions. *J. Am. Chem. Soc.* **2020**, *142*, 17693-17702; (e) Qiu, Y.; Scheremetjew, A.; Finger, L. H.; Ackermann, L. *Chem. Eur. J.* Electrophotocatalytic Undirected C−H Trifluoromethylations of (Het)Arenes. **2020**, *26*, 3241-3246; (f) Cowper, N. G. W.; Chernowsky, C. P.; Williams, O. P. Wickens, Z. K. Potent Reductants via Electron-Primed Photoredox Catalysis:

Unlocking Aryl Chlorides for Radical Coupling. *J. Am. Chem. Soc.* **2020**, *142*, 2093-2099; (g) Huang, H.; Strater, Z. M. Lambert, T. H. Electrophotocatalytic C−H Functionalization of Ethers with High Regioselectivity *J. Am. Chem. Soc.* **2020**, *142*, 1698-1703; (h) Kim, H.; Kim, H.; Lambert, T. H.; Lin, S. Reductive Electrophotocatalysis: Merging Electricity and Light to Achieve Extreme Reduction Potentials. *J. Am. Chem. Soc.* **2020**, *142*, 2087-2092; (i) Huang, H.; Lambert, T. H. Electrophotocatalytic S_NAr Reactions of Unactivated Aryl Fluorides at Ambient Temperature and Without Base. *Angew. Chem. Int. Ed.* **2020**, *59*, 658-662; (j) Zhang, W.; Carpenter, K. L.; Lin, S. Electrochemistry Broadens the Scope of Flavin Photocatalysis: Photoelectrocatalytic Oxidation of Unactivated Alcohols. *Angew. Chem. Int. Ed.* **2020**, *59*, 409-417; (k) Huang, H.; Strater, Z. M.; Rauch, M.; Shee, J.; Sisto, T. J.; Nuckolls, C.; Lambert, T. H. Electrophotocatalysis with a Trisaminocyclopropenium Radical Dication. *Angew. Chem. Int. Ed.* **2019**, *58*, 13318-13322; (l) Wang, F.; Stahl, S. S. Merging Photochemistry with Electrochemistry: Functional Group Tolerant Electrochemical Amination of C(sp^3)−H Bonds. *Angew. Chem. Int. Ed.* **2019**, *58*, 6385-6390; (m) Yan, H.; Hou, Z. W.; Xu, H.-C. Photoelectrochemical C−H Alkylation of Heteroarenes with Organotrifluoroborates. *Angew. Chem. Int. Ed.* **2019**, *58*, 4592-4595.

(6) Pause, L.; Robert, M.; Savéant, J.-M. Can Single-Electron Transfer Break an Aromatic Carbon-Hydrogen Bond in One Step? A Novel Example of Transition between Stepwise and Concerted Mechanisms in the Reduction of Aromatic Iodides. *J. Am. Chem. Soc.* **1999**, *121*, 7158-7159.

(7) For reductions of benzyl radicals to benzyl anions by PRC: (a) Donabauer, K. König, B. Strategies for the Photocatalytic Generation of Carbanion Equivalents for Reductant-Free C−C Bond Formations. *Acc. Chem. Res.* **2021**, *54*, 242-252. For examples of electrochemical reports: b) Zhang, W.; Lin, S. Electroreductive Carbofunctionalization of Alkenes with Alkyl Bromides via a Radical-Polar Crossover Mechanism. *J. Am. Chem. Soc.* **2020**, *142*, 20661-20670; (c) Lu, L.; Siu, J. C.; Lai, Y.; Lin, S. An Electroreductive Approach to Radical Silylation via the Activation of Strong Si−Cl Bond. *J. Am. Chem. Soc.* **2020**, *142*, 21272-21278. For the reduction potential of a benzyl radical: (d) J. Grimshaw, *Electrochemical Reactions and Mechanisms in Organic Chemistry*, Elsevier **2000**, pp. 89-157.

(8) The alkane product likely forms via high-voltage-mediated C=C bond reduction, see: Liu, X.; Liu, R.; Qiu, J.; Cheng, X.; Li, G. *Angew. Chem. Int. Ed.* **2020**, *59*, 13962-13967.

(9) For reviews on photosensitized TTET isomerizations of alkenes and its use in tandem strategies: (a) Molloy, J. J.; Morack, T.; Gilmour, R. Positional and Geometrical Isomerisation of Alkenes: The Pinnacle of Atom Economy. *Angew. Chem. Int. Ed.* **2019**, *58*, 13654-13664; (b) Yakubov, S.; Barham, J. P. Photosensitized direct C−H fluorination and trifluoromethylation in organic synthesis. *Beilstein J. Org. Chem.* **2020**, *16*, 2151-2192; (c) Fabry, D. C.; Ronge, M. A.; Rueping, M. Immobilization and Continuous Recycling of Photoredox Catalysis in Ionic Liquids for Applications in Batch Reactions and Flow Systems: Catalytic Alkene Isomerization by Using Visible Light. *Chem.-Eur. J.* **2014**, *21*, 5350-5354.

(10) We found Fe plate was a more robust material than RVC, less prone to mechanical shearing and gave a similar yield of **2a** (see SI).

(11) For reviews on electrode materials in organic electrochemistry: (a) Couper, A. M.; Pletcher, D.; Walsh, F. C. *Chem. Rev.* **1990**, *90*, 857-865; (b) Heard, D. M.; Lennox, A. J. J. *Angew. Chem. Int. Ed.* **2020**, *59*, 18866-18884.

(12) (a) Iqbal, J.; Srivastava, R. R. Cobalt(II) chloride catalyzed acylation of alcohols with acetic anhydride: scope and mechanism. *J. Org. Chem.* **1992**, *57*, 2001-2007; (b) Dabbagh, H. A.; Zamani, M. Catalytic conversion of alcohols over alumina-zirconia mixed oxides: Reactivity and selectivity. *Appl. Catal. A.* **2011**, *404*, 141-148. A method for selective elimination to form terminal olefins was reported but requires triphosgene: Ganiu, M. O.; Cleveland, A. H.; Paul, J. L.; Kartika, R. Triphosgene and DMAP as Mild Reagents for Chemoselective Dehydration of Tertiary Alcohols. *Org. Lett.* **2019**, *21*, 5611-5615.

(13) Our conditions retain C(sp^2)−O functionality, providing complementary selectivity to PRC reductions of aryl phosphinates: (a) Jin, S.; Dang, H. T.; Haug, G. C.; He, R.; Nguyen, V. D.; Nguyen, V. T.; Arman, H. D.; Schanze, K. S.; Larianov, O. V. Visible Light-Induced Borylation of C−O, C−N and C−X Bonds. *J. Am. Chem. Soc.* **2020**, *142*, 1603-1613; (b) Wang, S.; Wang, H.; König, B. Photo-induced thiolate catalytic activation of inert C_{aryl}−hetero bonds for radical borylation. *Chem* **2021**, ASAP, DOI: 10.1016/j.chempr.2021.04.016.

(14) Cole, J. P.; Chen, D.-F.; Kudisch, M.; Pearson, R. M.; Lim, C.-H.; Miyake, G. M. Organocatalyzed Birch Reduction Driven by Visible Light. *J. Am. Chem. Soc.* **2020**, *142*, 13573-13581.

(15) Chatterjee, A.; König, B. Birch-Type Photoreduction of Arenes and Heteroarenes by Sensitized Electron Transfer. *Angew. Chem. Int. Ed.* **2019**, *58*, 14289-14294.

(16) (a) Harirchian, B.; Bauld, N. L. Cation radical Diels-Alder cycloadditions in organic synthesis. A formal total synthesis of (−)-β-selinene. *J. Am. Chem. Soc.* **1989**, *111*, 1826-1828; (b) Liao, L.; Guo, R.; Zhao X. Organoselenium-Catalyzed Regioselective C−H Pyridination of 1,3-Dienes and Alkenes. *Angew. Chem. Int. Ed.* **2017**, 56, 3201-3205.

(17) (a) Lebel, H.; Davi, M.; Díez-González, S.; Nolan, S. P. Copper-Carbene Complexes as Catalysts in the Synthesis of Functionalized Styrenes and Aliphatic Alkenes. *J. Org. Chem.* **2007**, *72*, 144-149; (b) Level, H. Paquet, V. Rhodium-Catalyzed Methylenation of Aldehydes. *J. Am. Chem. Soc.* **2004**, *126*, 320-328.

(18) (a) Ganicz, T.; Stańczyk, W. Side-chain Liquid Crystal Polymers (SCLCP): Methods and Materials. An Overview. *Materials* **2009**, *2*, 95-128; b) Castruita, G.; García, V.; Arias, E.; Moggio, I.; Ziolo, R.; Ponce, A.; González, V.; Haley, J. E.; Flikkema, J. L.; Cooper T. Synthesis, optical and structural properties of sanidic liquid crystal (cholesteryl)benzoate-ethynylene oligomers and polymer. *J. Mat. Chem.* **2012**, 22, 3770-3780; (c) G. Misra, A. K. Srivastava, *Colloid and Polymer Science* **2008**, *286*, 445-451; K. Nilles, P. Theato, *Eur. Polym. J.* **2007**, *43*, 2901-2912.

(19) Conversion of a *p*-acetylbenzoate to a *p*-vinylbenzoate is been reported only as a low-yielding side reaction: Tayama, E.; Watanabe, K.; Sotome, S. Structural and mechanistic studies of the base-induced Sommelet-Hauser rearrangement of *N*-a-branched benzylic azetidine-2-carboxylic acid-derived ammonium salts. *Org. Biomol. Chem.* **2017**, *15*, 6668-6678.

(20) For transition metal catalyzed approaches: (a) Minato, A.; Suzuki, K. A remarkable steric effect in palladium-catalyzed Grignard coupling: regio- and stereoselective monoalkylation and -arylation of 1,1-dichloro-1-alkenes. *J. Am. Chem. Soc.* **1987**, *109*, 1257-1258; (b) Iwai, T.; Fujihara, T.; Terao, J.; Tsuji, Y. Iridium-Catalyzed Addition of Acid Chlorides to Terminal Alkynes. *J. Am. Chem. Soc.* **2009**, *131*, 6668-6669.

(21) K. Lam, I. E. Markó, Novel Electrochemical Deoxygenation Reaction using Diphenylphosphinates. *Org. Lett.* **2011**, *13*, 406-409.

(22) For full EPR investigations on **NpMI**$^{\bullet-}$, see SI.

(23) Demeter, A.; Bercés, T.; Biczók, L.; Wintgens, V.; Valat, P.; Kossanyi, J. Comprehensive Model of the Photophysics of *N*-Phenylnaphthalimides: The Role of Solvent and Rotational Relaxation. *J. Phys. Chem.* **1996**, *100*, 2001-2011.

(24) Strieth-Kalthoff, F.; James, M. J.; Teders, M.; Pitzer, L.; Glorius, F. Energy transfer catalysis mediated by visible light: principles, applications, directions. *Chem. Soc. Rev.* **2018**, *47*, 7190-7202.

(25) SET reduction of the *E*-isomer by **NpMI**$^{\bullet-*}$ cannot be ruled out, but redox potential differences between *E*-/*Z*- isomers are insufficient to provide high (>10:1) *Z*-selectivities. Previous literature for photoisomerism by closed-shell photocatalysts favors E_nT.

(26) See SI for full wavelength dependence experiments.

(27) For a relevant example, see: Zeman IV, C. J.; Kim, S.; Zhang, F.; Schanze, K. S. Direct Observation of the Reduction of Aryl Halides by a Photoexcited Perylene Diimide Radical Anion. *J. Am. Chem. Soc.* **2020**, *142*, 2204-2207. Calculated by the sums of ground state redox potentials (vs. SCE) and the tail of the UV-vis band at 490 nm (525 nm = 2.45 eV).

(28) In Ref. 14, formation of solvated electrons is proposed. Our reactions take place in non-alcoholic solvents. Formation of solvated electrons cannot rationalize reactivity differences between catalysts. Substrate-catalyst preassociation allows ultrashort lifetimes of excited photocatalyst doublet states to be circumvented.

(29) In Ref. 30, an attempt to determine the lifetime of ^{2}[*N*-arylnaphthalimide$^{\bullet-*}$] in MeCN by transient absorption spectroscopy led to rapid bleaching, suggesting solvent redox processes.

(30) Gosztola, D.; Niemczyk, M. P.; Svec, W.; Lukas, A. S.; Wasielewski, M. R. Excited Doublet States of Electrochemically Generated Aromatic Imide and Diimide Radical Anions. *J. Phys. Chem. A* **2000**, *104*, 6545-6551.

(31) π-stacking interactions were implicated by DFT to explain selective reduction of arenes over aliphatic esters by photoexcited neutral electron donors: Doni, E.; Mondal, B.; O'Sullivan, S.; Tuttle, T.; Murphy, J. A. Overturning Established Chemoselectivities: Selective Reduction of Arenes over Malonates and Cyanoacetates by Photoactivated Organic Electron Donors. *J. Am. Chem. Soc.* **2013**, 135, 10934-10937.

(32) Hunter and Sanders claimed that π-π stacking rarely leads to notable UV-vis perturbations. Instead, σ-π interactions occur favoring edge-to-face binding: Hunter, C. A.; Sanders, J. K. M. The Nature of π-π Interactions. *J. Am. Chem. Soc.* **1990**, *112*, 5525-5534.

(33) (a) Barham, J. P.; Coulthard, G.; Kane, R. G.; Delgado, N.; John, M. P.; Murphy, J. A. Double Deprotonation of Pyridinols Generates Potent Organic Electron-Donor Initiators for Haloarene-Arene Coupling. *Angew. Chem. Int. Ed.* **2016**, *55*, 4492-4496; (b) Barham, J. P.; Coulthard, G.; Emery, K. J.; Doni, E.; Cumine, F.; Nocera, G.; John, M. P.; Berlouis, L. E. A.; McGuire, T.; Tuttle, T.; Murphy, J. A. KO*t*Bu: A Privileged Reagent for Electron Transfer Reactions? *J. Am. Chem. Soc.* **2016**, *138*, 7402-7410.

(34) Selected reviews: a) Lima, C. G. S.; de M. Lima, T.; Duarte, M.; Jurberg, I. D.; Paixão, M. W. Organic Synthesis Enabled by Light-Irradiation of EDA Complexes: Theoretical Background and Synthetic Applications. *ACS Catal.* **2016**, *6*, 1389-1407; b) Crisenza, G. E. M.; Mazzarella, D.; Melchiorre, P. Synthetic Methods Driven by the Photoactivity of Electron Donor Acceptor Complexes. *J. Am. Chem. Soc.* **2020**, *142*, 5461-5476.

(35) Bhattacharyya, A.; De Sarkar, S.; Das, A. Supramolecular Engineering and Self-Assembly Strategies in Photoredox Catalysis. *ACS Catal.* **2021**, *11*, 710-733.

(36) Selected examples: a) Berg, N.; Bergwinkl, S.; Nuernberger, P.; Horinek, D.; Gschwind, R. M. Extended Hydrogen Bond Networks for Effective Proton-Coupled Electron Transfer (PCET) Reactions: The Unexpected Role of Thiophenol and Its Acidic Channel in Photocatalytic Hydroamidations. *J. Am. Chem. Soc.* **2021**, *143*, 724-735; b) Burg, F.; Bach, T. Lactam Hydrogen Bonds as Control Elements in Enantioselective Transition-Metal-Catalyzed and Photochemical Reactions. *J. Org. Chem.* **2019**, *84*, 8815-8836.

(37) Selected examples: a) Giedyk, M.; Narobe, R.; Weiß, S.; Touraud, D.; Kunz, W.; König, B. Photocatalytic activation of alkyl chlorides by assembly-promoted single electron transfer in microheterogeneous solutions. *Nat. Catal.* **2020**, *3*, 40-47; b) Kaur, J.; Shahin, A.; Barham, J. P. Photocatalyst-Free, Visible-Light-Mediated C(sp^3)−H Arylation of Amides via a Solvent-Caged EDA Complex. *Org. Lett.* **2021**, *23*, 2002-2006.

Contents Graphic